Front. Phys. China, 2007, 2(4): 403－409
DOI 10.1007/s11467-007-0051-2

REVIEW ARTICLE

NIU Yue-ping, QIAN Jun, FENG Xun-li, GONG Shang-qing

Enhancement of Kerr nonlinearity and its application to entangled state discrimination

Abstract In this paper, the recent research on the enhanced Kerr nonlinearity and its application in entangled state discrimination is reported. Two kinds of dynamics, including interacting double dark resonances and spontaneously generated coherence, are presented to enhance the Kerr nonlinearity. The application of Kerr nonlinearity in quantum state discrimination is also discussed. An arbitrary Greenberger-Horne-Zeilinger state can be discriminated using two-photon polarization parity detection which resorts to cross-Kerr nonlinearity between a single-photon qubit and probe field. In addition, a scheme for Greenberger-Horne-Zeilinger state discrimination of matter qubits is also proposed using the dipole induced transparency in a cavity-dipole system.

Keywords Kerr nonlinearity, dark resonance, entangled state discrimination

PACS numbers 42.65.-k, 03.65.Ud

1 Introduction

Because the optical nonlinear susceptibilities play important roles in such areas as frequency conversion [1], generation of optical solitons [2, 3] and polarization phase gate [4], etc., it is desirable for people to have large nonlinear susceptibilities under conditions of low light power [5–8]. In the domain of quantum information, for example, the cross-Kerr nonlinearity can be engaged to realize two-photon polarization detection, optical Controlled-NOT gate [9], high-efficiency quantum-nondemolition (QND) single-photon-number-resolving detector [10], symmetry nondestructive Bell-state detection [11], and so on. In order to enhance the Kerr nonlinearity, several schemes have been proposed [12–14]. For instance, Schmidt and Imamoglu proposed a four-level *N*- configuration system to enhance the Kerr nonlinearity where the ideal electromagnetically induced transparency (EIT) regime is disturbed by an additional off-resonant level. Nakajima found that the autoionizing resonance could lead to the enhanced third-order susceptibility with zero absorption. In the present paper, two schemes are first given to enhance the Kerr nonlinearity, then its application in entangled states discrimination through cross-phase modulation is taken into consideration.

NIU Yue-ping, QIAN Jun, FENG Xun-li, GONG Shang-qing (✉)
State Key Laboratory of High Field Laser Physics, Shanghai Institute of Optics and Fine Mechanics, Chinese Academy of Sciences, Shanghai 201800, China
E-mail: sqgong@mail.siom.ac.cn

Received June 20, 2007

2 Giant enhancement of Kerr nonlinearity

2.1 Via interacting double dark resonances

In the generic four-level lambda-type system as shown in Fig. 1, a resonant coupling laser of Rabi frequency Ω_s couples levels $|2\rangle$ and $|3\rangle$, while a weaker probe beam with Rabi frequency Ω_p couples levels $|1\rangle$ and $|2\rangle$. Therefore, a simple lambda-type configuration is formed. The resulting-dark state is coherently coupled to another metastable state

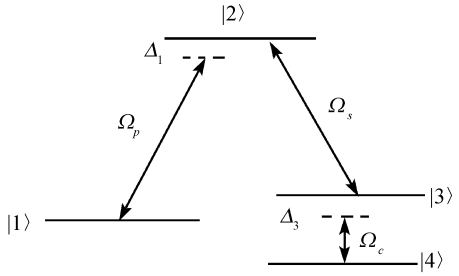

Fig. 1 A generic four-level Λ-type system with a twofold level structure.

$|4\rangle$ by a microwave or quasistatic field Ω_c, hence, the double dark resonances appear [15].

The perturbative and iterative methods are adopted, then the density matrix equations are solved and the analytical expressions of the first- and third-order susceptibilities are ultimately given as [16]

$$\chi^{(1)} = \frac{-2N|\mu_{12}|^2}{\varepsilon_0\hbar} \cdot \frac{2(\Delta_2^1 - \Delta_1\Delta_3 - \Omega_c^2)}{\Delta_1^3 + \mathrm{i}\Delta_1^2(r+\mathrm{i}\Delta_3) - \mathrm{i}r\Omega_c^2 + \Delta_3\Omega_s^2 + \Delta_1(-\mathrm{i}r\Delta_3 - \Omega_c^2 - \Omega_s^2)} \tag{1}$$

$$\chi^{(3)} = \frac{-2N|\mu_{12}|^4}{3\varepsilon_0\hbar^3} \cdot \frac{1}{[(-\mathrm{i}r+\Delta_1)(\Delta_1^2 - \Delta_1\Delta_3 - \Omega_c^2) - (\Delta_1 - \Delta_3)\Omega_s^2]} \cdot \left\{ \frac{2\Omega_s^2\Omega_c^2(-\Delta_1\Delta_3 + \Delta_3^2 + \Omega_c^2)}{[-\mathrm{i}(r-\mathrm{i}\Delta_1)(\Delta_1^2 - \Delta_1\Delta_3 - \Omega_c^2) + (\Delta_1 - \Delta_3)\Omega_s^2]^2} - \frac{(\Delta_1^2 - \Delta_1\Delta_3 - \Omega_c^2)^3[\Delta_3^2 + 2(r^2 + \Omega_c^2)]}{[(\mathrm{i}r+\Delta_1)(\Delta_1^2 - \Delta_1\Delta_3 - \Omega_c^2)\Omega_s - (\Delta_1 - \Delta_3)\Omega_s^3]^2} + [(\Delta_1(-\Delta_1 + \Delta_3) + \Omega_c^2)^2[-\mathrm{i}(r - 13\mathrm{i}\Delta_1)(\Delta_1 - \Delta_3) + 12\Omega_c^2) - 2\Delta_1(\Delta_1 - \Delta_3)^3\Omega_s^2] / [(\mathrm{i}r+\Delta_1)(\Delta_1^2 - \Delta_1\Delta_3 - \Omega_c^2) - (\Delta_1 - \Delta_3)\Omega_s^2]^{-2} \right\} \tag{2}$$

where $\chi = \chi^{(1)} + 3|E_p|^2\chi^{(3)}$ is utilized. γ is assumed to be the decay rate of the exited level $|2\rangle$ to the other levels and all the other parameters are scaled by it.

Lukin *et al*. [15] pointed out that the coherent control field Ω_c caused the occurrence of two distinct dark resonances, the interaction of which resulted in a strong absorption. The position and width of the absorption line can be engineered by properly tuning the coherent control field. This feature can be reproduced from the above expression of $\chi^{(1)}$. Here, the focus is on the third-order susceptibility through the numerical simulation. It is first considered that the coherent control field is on-resonance, i.e., $\Delta_3 = 0$. Setting $\Omega_s = \gamma$ and $\Omega_c = 0.2\gamma$, the variation of the refractive part of the third-order susceptibility is displayed in Fig. 2(a) (*solid line*). Compared with the conventional three-level lambda-type system without the control field Ω_c [*dash-dotted line* in Fig. 2(a)], $\mathrm{Re}[\chi^{(3)}]$ is now enhanced by about two orders of magnitude in the vicinity of the resonance. Nevertheless, the enhanced $\mathrm{Re}[\chi^{(3)}]$ and the strong absorption are now superposed, as shown in Fig. 2(a) (*dotted line*). That is, although the Kerr nonlinearity is enhanced dramatically, it is accompanied by a strong linear absorption. This is not desired in the applications of low-level intensity nonlinear optics. Fortunately, this case varies with the control field tuning, which makes the enhanced $\mathrm{Re}[\chi^{(3)}]$ with vanishing absorption possible.

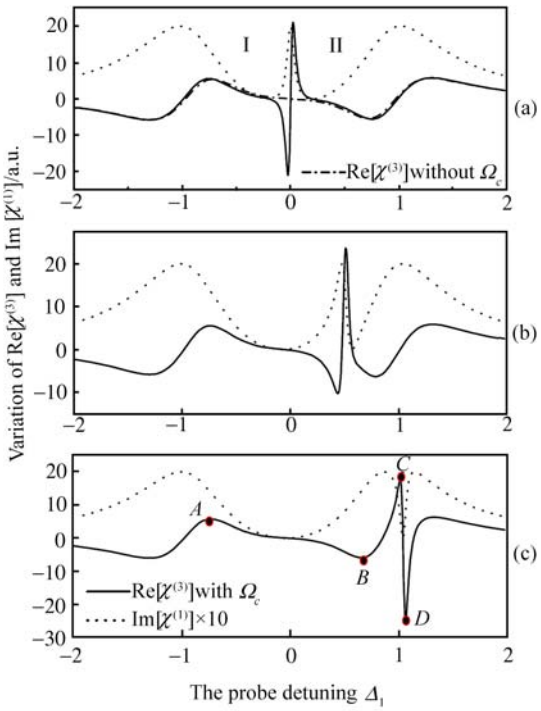

Fig. 2 Variation of $\mathrm{Re}[\chi^{(3)}]$ (*solid line*) and $\mathrm{Im}[\chi^{(1)}]$ (*dotted line*) as a function of Δ_1. Parameters are $\Omega_s = \gamma$, $\Omega_c = 0.2\gamma$, and $\Delta_3 = 0.0$ **(a)**, $\Delta_3 = 0.5\gamma$ **(b)**, $\Delta_3 = \gamma$ **(c)**.

When the coherent control field is detuned, the magnitude and position of the enhanced $\mathrm{Re}[\chi^{(3)}]$, together with the linear absorption, vary. Figure 2 exhibits the variation process. With the increase in the detuning Δ_3, the two distinct EIT windows become different: one broadens (region I) while the other narrows (region II). When Δ_3 changes from 0 to γ, it is surprising to see that the enhanced $\mathrm{Re}[\chi^{(3)}]$ gradually enters into the narrower EIT window. It is clearly seen from Fig. 2(c) that the Kerr nonlinearity is dramatically enhanced with suppressed linear absorption (region II). Because $\mathrm{Im}[\chi^{(1)}]$ and $\mathrm{Re}[\chi^{(3)}]$ of the conventional lambda type EIT system are just the same as those shown in region I, a comparison between the present scheme and the single dark resonance system could be drawn by analyzing the two regions. In region I, for certain probe detunings (dots *A* and *B*), the enhanced $\mathrm{Re}[\chi^{(3)}]$ [17] is accompanied by fractional linear absorption. In region II, however, the giant enhanced $\mathrm{Re}[\chi^{(3)}]$ (dots *C* and *D*) corresponds to the vanishing absorption. This striking contrast implies the principal result of the present paper. Compared with the single dark

resonant case, the interacting double dark resonances cause giant enhancement of the Kerr nonlinearity with the vanishing linear absorption. In the dressed state picture, this case corresponds to the profound interference situation because the eigenvalues of two of the dressed states intersect [15].

It can be found from the analytical expression of $\chi^{(3)}$ that the first term of Eq. (2) is proportional to the product of the two fields Ω_s and Ω_c, while the other two terms are independent of the product. If the first term and the other two are marked as $T_1(\Omega_s\Omega_c)$ and $T_{2,3}$ respectively, then $\chi^{(3)} = T_1(\Omega_s\Omega_c) + T_{2,3}$. A comparison between $\mathrm{Re}[T_1]$ and $\mathrm{Re}[\chi^{(3)}]$ is shown in Fig. 3. Obviously, it can be seen that they are approximately coincident in the narrow region of giant enhancement of the Kerr nonlinearity. As a result, it is considered from the analytical aspect that the giant enhancement of the third-order susceptibility is undoubtedly caused by the interaction between Ω_s and Ω_c. In other words, the Kerr nonlinearity is greatly enhanced by the interacting double dark states. As for the scheme proposed by Schmidt and Imamoglu [18], there exists only one dark state, and no interaction arises although *N*-type multilevel is applied. Thus, a new possibility is proposed here for giant enhancement of Kerr nonlinearity by interacting double dark resonances.

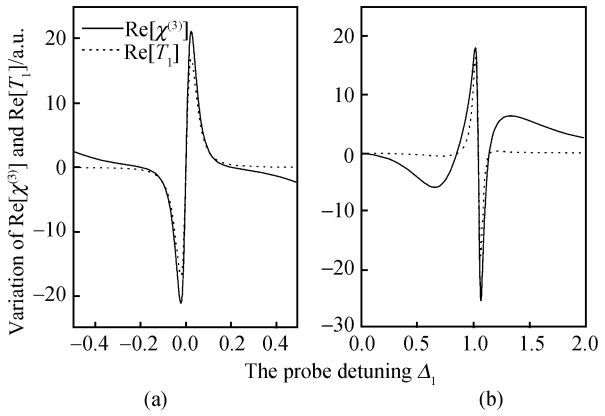

Fig. 3 Variation of $\mathrm{Re}[\chi^{(3)}]$ (*solid line*) and $\mathrm{Re}[T_1]$ (*dotted line*) versus Δ_1. Parameters are $\Omega_s = \gamma$, $\Omega_c = 0.2\gamma$, and **(a)** $\Delta_3 = 0.0$, **(b)** $\Delta_3 = \gamma$.

2.2 Via spontaneously generated coherence (SGC)

The effect of SGC [19] has led to various interesting phenomena that have potential uses [20–23]. In atomic systems, although it is difficult to realize SGC experimentally in free space, several proposals have been put forward to simulate such an effect [24]. The effect of SGC occurs in atomic, molecular or semiconductor quantum dot systems could have useful applications in laser physics and other areas of quantum optics. In the following part, the effect of SGC on the enhancement of the Kerr nonlinearity in the popularly discussed lambda-type three-level system is presented.

As shown in Fig. 4, a resonant coupling field Ω_c drives the transition between levels $|1\rangle$ and $|2\rangle$ while a probe field Ω_p is applied to the transitions $|1\rangle$ and $|3\rangle$. When the two lower levels $|2\rangle$ and $|3\rangle$ are closely spaced so that the two transitions to the excited state interact with the same vacuum mode, SGC could be presented. Under the rotating wave approximation, the systematic density matrix in the interaction picture involving the SGC can be written as

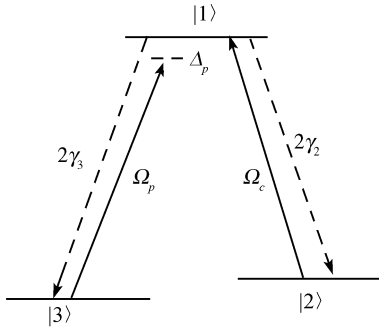

Fig. 4 Schematic energy-level diagrams showing the lambda-type system with the coupling field Ω_c, the probe field Ω_p and the decay rates $2\gamma_2$ and $2\gamma_3$.

$$
\begin{aligned}
\dot{\rho}_{11} &= -2(\gamma_2+\gamma_3)\rho_{11} + \mathrm{i}\Omega_p(\rho_{31}-\rho_{13}) + \mathrm{i}\Omega_c(\rho_{21}-\rho_{12}) \\
\dot{\rho}_{33} &= 2\gamma_3\rho_{11} + \mathrm{i}\Omega_p(\rho_{13}-\rho_{31}) \\
\dot{\rho}_{23} &= -\mathrm{i}\Delta_p\rho_{23} + 2p\sqrt{\gamma_2\gamma_3}\rho_{11} + \mathrm{i}\Omega_c\rho_{13} - \mathrm{i}\Omega_p\rho_{21} \\
\dot{\rho}_{13} &= -(\gamma_2+\gamma_3+\mathrm{i}\Delta_p)\rho_{13} - \mathrm{i}\Omega_p(\rho_{11}-\rho_{33}) + \mathrm{i}\Omega_c\rho_{23} \\
\dot{\rho}_{12} &= -(\gamma_2+\gamma_3)\rho_{12} + \mathrm{i}\Omega_p\rho_{32} - \mathrm{i}\Omega_c(\rho_{11}-\rho_{22})
\end{aligned}
\qquad (3)
$$

The above equations are constrained by $\rho_{11}+\rho_{22}+\rho_{33}=1$ and $\rho_{ji}^{*} = \rho_{ij}$. $\Delta_p = \omega_{13} - \omega_p$ which means the detuning of the probe field from the optical transition. The effect of SGC is very sensitive to the orientations of the atomic dipole moments $\boldsymbol{\mu}_{12}$ and $\boldsymbol{\mu}_{13}$. Here, the parameter p denotes the alignment of the two dipole moments and is defined as $p = \boldsymbol{\mu}_{12}\cdot\boldsymbol{\mu}_{13} / |\boldsymbol{\mu}_{12}\cdot\boldsymbol{\mu}_{13}|$. The terms with $p\sqrt{\gamma_2\gamma_3}$ represent the quantum interference results from the cross coupling between spontaneous emission paths $|1\rangle - |2\rangle$ and $|1\rangle - |3\rangle$. With the restriction that each field acts only on one transition, Rabi frequencies $\Omega_{c(p)} = \Omega_{c(p)}^{0}\sqrt{1-p^2}$. It should be noted that only for small energy spacing between the two lower levels are the interference terms in Eq. (3) significant, otherwise, the oscillatory terms will average out to zero and thereby the effect of SGC vanishes.

According to the above discussion, under the weak-probe approximation, the matrix element ρ_{13} can be solved up to the third-order, hence the first- and third-order susceptibilities $\chi^{(1)}$ and $\chi^{(3)}$ could be expressed as

$$\chi^{(1)} = \frac{-2N|\boldsymbol{\mu}_{13}|^2}{\varepsilon_0\hbar\Omega_p}\rho_{13}^{(1)} = \frac{-2N|\boldsymbol{\mu}_{13}|^2}{\varepsilon_0\hbar}\frac{\Delta_p}{\Omega_c^2 + \mathrm{i}(\gamma_2+\gamma_3+\mathrm{i}\Delta_p)\Delta_p} \tag{4}$$

$$\begin{aligned}\chi^{(3)} &= \frac{-2N|\boldsymbol{\mu}_{13}|^4}{3\varepsilon_0\hbar^3\Omega_p^3}\rho_{13}^{(3)} \\ &= \frac{-2N|\boldsymbol{\mu}_{13}|^4}{3\varepsilon_0\hbar^3}\{4\mathrm{i}\Omega_c^4 p^2\gamma_2(\gamma_2+\gamma_3)\Delta_p^2(\Omega_c^2-\Delta_p^2) \\ &+\Delta_p[\Omega_c^2+\mathrm{i}(\gamma_2+\gamma_3+\mathrm{i}\Delta_p)\Delta_p] \\ &\cdot[\Omega_c^2-\mathrm{i}(\gamma_2+\gamma_3-\mathrm{i}\Delta_p)\Delta_p] \\ &\cdot[2\Omega_c^4\gamma_3-\mathrm{i}\Omega_c^2\gamma_2(\gamma_2+\gamma_3)\Delta_p \\ &+\Delta_p^2(3\Omega_c^2\gamma_2+\gamma_2\gamma_3^2+\gamma_2^3+2\gamma_3(\Omega_c^2+\gamma_2^2))]\}/\beta\end{aligned} \tag{5}$$

with

$$\begin{aligned}\beta &= \gamma_3[\Omega_c^3-\mathrm{i}\Omega_c(\gamma_2+\gamma_3-\mathrm{i}\Delta_p)\Delta_p]^2 \\ &\cdot[\Omega_c^2+\mathrm{i}(\gamma_2+\gamma_3+\mathrm{i}\Delta_p)\Delta_p]^3\end{aligned} \tag{6}$$

According to the Eqs. (4) and (5), the linear absorption (*dotted curve*) and the refractive part of the third-order susceptibility (*solid curve*) are shown in Fig. 5 as a function of the probe detuning. For simplicity, all the parameters are scaled by the decay rate γ_2, $\Omega_c^0 = 4\gamma_2$ and $\gamma_3 = \gamma_2$. It can be seen from Fig. 5 that when $p = 0$ (no interference between spontaneous emission channels) a couple of general linear absorption and Kerr nonlinearity curves occur [17]. With the presence of spontaneous emission interference, the refractive part of the third-order susceptibility enhances as well as the EIT window narrows [25]. However, for large values of *p*, the refractive part of the third-order susceptibility builds up evidently. It is clearly to be seen that the maximal Kerr nonlinearity of *p*=0.99 is about six times that of *p*=0. In addition, although the EIT window narrows, the maximal Kerr nonlinearity enters the EIT window gradually; therefore, the corresponding linear absorption becomes negligible. On the other hand, the nonlinear absorption $\mathrm{Im}[\chi^{(3)}]$ is also presented in Fig. 5 (*dash-dotted curve*). It is noted that the variation of the nonlinear absorption with the SGC is very similar to that of the linear absorption. The enhanced Kerr nonlinearity gradually enters the "nonlinear EIT window" and the ratio of the real and imaginary part of $\chi^{(3)}$ improves significantly when the SGC intensifies from *p*=0 to *p*=0.99. This means that in the case of optimal SGC, both enhanced Kerr nonlinearity and negligible linear and nonlinear absorptions can be realized simultaneously.

An inspection of $\rho_{ij}^{(m)}(i,j=1,2,3;m=1,2,3)$ is made in order to get a qualitative explanation for the above numerical results [26]. It is found that the density matrix element $\rho_{23}^{(2)}$ is an extra term introduced by SGC. This term accordingly makes the third-order susceptibility acquire an additional term associated with SGC. The analytical expression $\rho_{13}^{(3)}$ shows that the first term is the product of the coupling field and the additional term. That is to say, in the present lambda-type system, the spontaneous decays from the upper state to the lower closely spaced levels interfere and give rise to an extra coherence between the two lower levels [27，28]. Thereby, the coupling field interacts with this extra coherence, thus the Kerr nonlinearity is evidently enhanced. Figure 6 shows the coherence term $|\rho_{23}^{(2)}|$ as a function of the probe detuning with different SGC. It is obvious that the stronger the SGC is, the more remarkable the coherence becomes. Hence, the enhancement of the Kerr nonlinearity is attributed to the extra coherence between the two lower levels induced by SGC.

Apparently, the generalization to the ladder and *V*-type three level systems is straightforward [26]. Especially it is noted in the *V*-type system that the Kerr nonlinearity can be manipulated to buildup dramatically at the exact point of

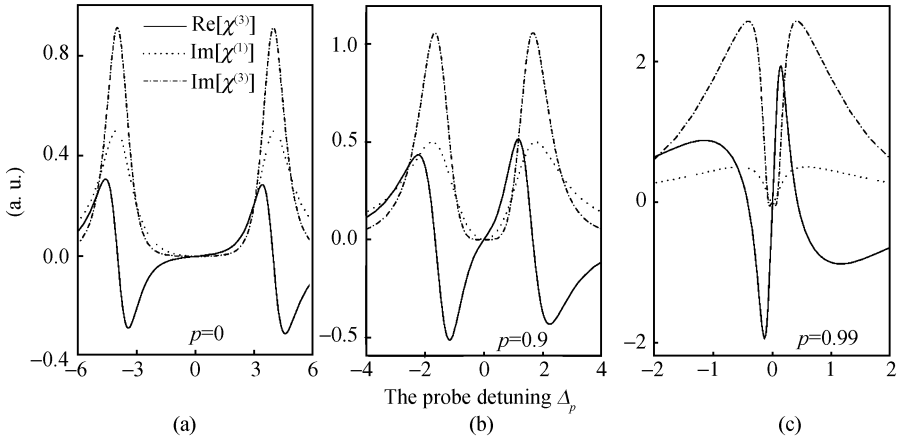

Fig. 5 Kerr nonlinearity $\mathrm{Re}[\chi^{(3)}]$ (*solid curve*), linear absorption $\mathrm{Im}[\chi^{(1)}]$ (*dotted curve*) and nonlinear absorption $\mathrm{Im}[\chi^{(3)}]$ (*dash-dotted curve*) of the lambda-type system with different SGC. Parameters are $\Omega_c^0 = 4.0\gamma_2$ and $\gamma_3 = 1.0\gamma_2$.

zero linear absorption.

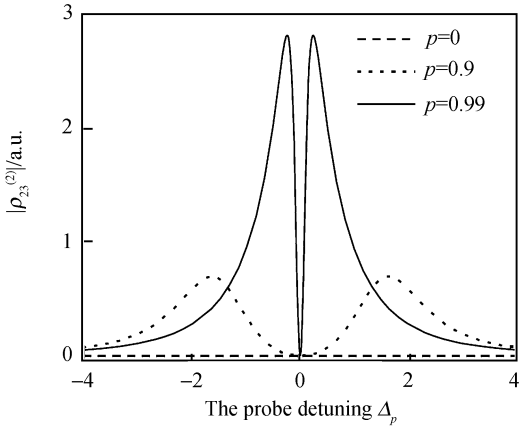

Fig. 6 Extra coherence term $\left|\rho_{23}^{(2)}\right|$ as a function of the probe detuning with different SGC. Parameters are the same as Fig. 5.

3 Greenberger-Horne-Zeilinger states discrimination of photonic and atomic qubits

It is well known that an entangled state is an indispensable resource which is widely applied in many aspects such as quantum key distribution and quantum logic gates. Greenberger-Horne-Zeilinger (GHZ) state is one of the most important multi-particle entangled states for quantum information processing. On many occasions, one needs to discriminate GHZ states to post-select relevant quantum operations to complete a given task. A GHZ state analyzer has been proposed to identify two typical GHZ states from other variations under local single-qubit flip operation using linear-optics elements [29]. A novel scheme is presented to distinguish all universal GHZ states of photonic qubits in the regime of practical weak nonlinearity at the present state of the art experimentally [30]. Cross-Kerr nonlinearity is engaged to realize two-photon polarization detection which is a key building block. A scheme for GHZ state discrimination of atomic qubits is also proposed using dipole induced transparency (DIT) in a cavity-dipole system [31]. The extension to *N*-particle cases of our proposals is straightforward. They are useful for quantum error correction, quantum secret key sharing and quantum state tomography.

Universal three-particle GHZ states are given by

$$\begin{aligned}
\left|\Phi_1^{\pm}\right\rangle &= \frac{1}{\sqrt{2}}(\left|111\right\rangle \pm \left|000\right\rangle)\\
\left|\Psi_1^{\pm}\right\rangle &= \frac{1}{\sqrt{2}}(\left|011\right\rangle \pm \left|100\right\rangle)\\
\left|\Psi_2^{\pm}\right\rangle &= \frac{1}{\sqrt{2}}(\left|101\right\rangle \pm \left|010\right\rangle)\\
\left|\Psi_3^{\pm}\right\rangle &= \frac{1}{\sqrt{2}}(\left|110\right\rangle \pm \left|001\right\rangle)
\end{aligned} \tag{7}$$

where $|1\rangle$ and $|0\rangle$ are qubit states which can be photonic polarizations and stable atomic levels. Apparently, these maximally entangled states are equivalent under local (single-particle) spin-flip operations.

Before making the detailed discussion, the QND parity detector is first recalled using weak Kerr nonlinearity [9]. Two photonic qubits are initially prepared in the even parity states $\{|HH\rangle$ and $|VV\rangle\}$ or the odd parity states $\{|HV\rangle$ and $|VH\rangle\}$, where *H*/*V* denotes horizontal/vertical polarization state, and the probe beam is initially prepared in a coherent state $|\alpha\rangle_p$. Polarizing beam splitter (PBS) transmits the horizontal polarizing photons and reflects the vertical polarizing ones. The action of the PBSs and Kerr-nonlinearity evolves the combined system $|\psi\rangle|\alpha\rangle_p$ ($|\psi\rangle = |HH\rangle$, $|VV\rangle$, $|HV\rangle$, or $|VH\rangle$) to $|HH\rangle|\alpha\rangle_p$, $|VV\rangle|\alpha\rangle_p$, $|HV\rangle|\alpha e^{i\theta}\rangle_p$, or $|VH\rangle|\alpha e^{-i\theta}\rangle_p$ respectively. No phase shift of the probe beam arises when the input state is the even parity state, while the opposite sign phase shifts $\pm\theta$ occur in the case of the odd parity state. Then, the homodyne measurement is performed to split the even parity states from the odd parity ones. When the local oscillator phase $\pi/2$ offset from the probe beam is chosen, the states $|\alpha e^{\pm i\theta}\rangle_p$ cannot be distinguished. Thus, the appropriate homodyne measurement allows us to distinguish the even states from the odd ones. It is worth noting that nearly deterministic discrimination is possible as long as the requirement $\alpha\theta^2 \gg 1$ is satisfied. It means that the parity detector can be experimentally realized in the weak cross-Kerr nonlinearity regime, provided the amplitude of the probe beam is sufficiently large.

The 3-photon GHZ state analyzer is depicted in Fig. 7. Entangled photons enter the analyzer from input ports A, B and C. Parity detectors PD_{AB} and PD_{AC} can nondestructively measure the parity of two photons which use the cross-Kerr nonlinearity between the single-photons and weak coherent light. Then, the photons go through half-wave planes (HWP) and PBS, and then are detected by common photon detectors. Obviously, $|\Phi^{\pm}\rangle$ and $|\Psi_3^{\pm}\rangle$ can be distinguished from $|\Psi_1^{\pm}\rangle$ and $|\Psi_2^{\pm}\rangle$ by the first parity detector PD_{AB} because the former two are the even parity for A and B photons, thus no phase shifts arise in the probe beam. In the same way, $|\Phi^{\pm}\rangle$ and $|\Psi_2^{\pm}\rangle$ can also be separated from $|\Psi_1^{\pm}\rangle$ and $|\Psi_3^{\pm}\rangle$ by the second parity detector PD_{AC}. According to the measurement results of two parity detectors, the eight universal GHZ states are divided into four classes. Each class can be further discriminated with the help of HWP, PBS and the coincidence between the six detectors. After passing through HWPs, each photon undergoes a $\pi/4$ rotation of the polarization, i.e., $H\rightarrow H+V$, $V\rightarrow H-V$ (here and in what follows the normal coefficients are ignored for clarity). The relative phase between $|\Psi_i^{\pm}\rangle$ with threefold coincidences of photon detectors D_{H/V_i} (i = 1, 2, 3). For example, the initial state $|\Psi_1^{\pm}\rangle$ evolves to

$$\begin{aligned}|\Psi_1^+\rangle &\xrightarrow{\text{HWP}} |HHH\rangle - |HVV\rangle - |VHV\rangle + |VVH\rangle \\ |\Psi_1^-\rangle &\xrightarrow{\text{HWP}} |VHH\rangle + |HVH\rangle - |HHV\rangle - |VVV\rangle\end{aligned} \quad (8)$$

Apparently, $|\Psi_1^+\rangle$ leads to coincidences between detectors D_{H_1}, D_{H_2} and D_{H_3} (or $H_1V_2V_3$, $V_1H_2V_3$ and $V_1V_2H_3$); on the other hand, the initial state $|\Psi_1^-\rangle$ leads to coincidences between detectors D_{H_1}, D_{H_2} and D_{V_3} (or $H_1V_2H_3$, $V_1H_2H_3$ and $V_1V_2V_3$). In other words, behind the HWPs, $|\Psi_i^+\rangle$ results in one or three horizontally, and zero or two vertically polarized photons, while $|\Psi_i^-\rangle$ results in zero or two vertically, and one or three horizontally polarized photons. Large nonlinear phase shift is not necessary provided that the strength of coherent field in the parity detection is strong enough.

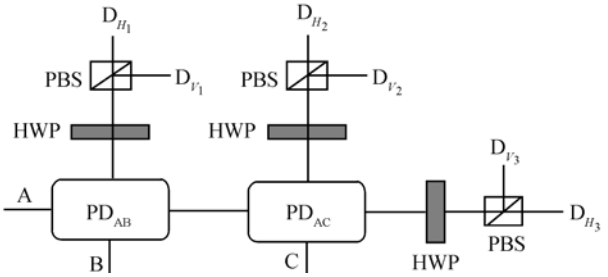

Fig. 7 GHZ state analyzer using weak nonlinearity.

A 3-atom GHZ state analyzer, as shown in Fig. 8, is discussed as below. Each cavity contains a single trapped atom and is evanescently coupled to up-and-down waveguides. An atom has an excited state $|e\rangle$ and two ground states $|g\rangle$ and $|m\rangle$. One can determine whether the states of two atoms are the same or different using DIT in which the coherent field is measured by detectors and the states of the atoms do not change [32]. Universal GHZ states for three atoms have the similar forms of Eq. (7), but here qubits states change to atomic states $|g\rangle$ and $|m\rangle$. A two-step strategy is adopted to fulfill the analysis of the universal GHZ states: (1) The four classes of GHZ states can be distinguished from each other only through two DIT parity measurements [see Fig. 8(a)]; (2) A single-qubit rotation and a parity check of the three atoms are used to separate the two states in each class with the relevant phase π [see Fig. 8(b)]. In the first step, DIT is utilized to measure the parities of the dipoles in C_1 and C_2 as well as in C_2 and C_3, respectively. For the first parity measurement, two mirrors are inserted into the optical path to guide the probe beam $|\alpha\rangle_1$ to the detectors D_1 and D_4 and avoid the coupling between $|\alpha\rangle_1$ and the cavity C_3. Then, for the second parity measurement, the mirrors are removed and the probe beam $|\alpha\rangle_2$ is input just before the cavity C_2. The single-qubit rotation can be realized in two-photon Raman transition configuration. When the detuning between two optical fields and the corresponding atomic transitions are much larger than the spontaneous emission rate of the atomic level $|e\rangle$, the fidelity of the single-qubit operations is nearly 100 %.

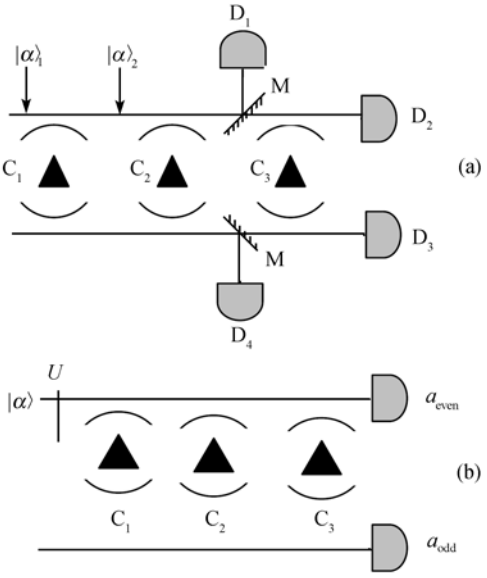

Fig. 8 GHZ state analyzer using dipole induced transparency.

4 Conclusion

Two schemes on the enhancement of the Kerr nonlinearity and its application in the discrimination of entangled states are reviewed. The Kerr nonlinearity enhanced by the interacting dark resonances can be several orders of magnitude larger than that generated in a single dark resonance system. Due to SGC, the Kerr nonlinearity of general discussed three-level atomic system can be enhanced while maintaining vanishing linear and nonlinear absorptions under proper parameter conditions. Two different schemes are presented to distinguish all universal GHZ states, in the regime of weak Kerr nonlinearity and DIT of the cavity-dipole system, respectively. They are essential for the quantum error correction, quantum secret key sharing and quantum state tomography.

References

1. Harris S. E., Field J. E., and Imamoglu A., Phys. Rev. Lett.,1991, 64: 1107
2. Tikhonenko V., Christou J., and Luther-Davies B., Phys. Rev. Lett.,1996, 76: 2698
3. Wu Y. and Deng L., Phys. Rev. Lett., 2004,93: 143904
4. Rebic S., Vitali D., Ottaviani C., Tombesi P., Artoni M., Cataliotti F., and Corbalan R., Phys. Rev. A,2004, 70: 032317
5. Harris S., Phys. Today,1997, 50 (7): 36
6. Schmidt H. and Imamoglu A., Opt. Lett.,1996, 21: 1936
7. Hoonsoo Kang and Yifu Zhu, Phys. Rev. Lett.,2003, 91: 093601

8. Matsko, A. B.,et al., Opt. Lett., 2003, 28: 96
9. Nemoto K. and Munro W. J., Phys. Rev. Lett., 2004, 93: 250502
10. Munro W. J., Kae Nemoto, Beausoleil R. G., and Spiller T. P., Phys. Rev. A, 2005, 71: 033819
11. Barrett S. D., Pieter Kok, Kae Nemoto, Beausoleil R. G., Munro W. J., and Spiller T. P., Phys. Rev. A, 2005, 71: 060302
12. Schmidt H. and Imamoglu A., Opt. Lett.,1996, 21: 1936
13. Matsko A. B., Novikova I., Welch G. R., and Zubairy M. S., Opt. Lett., 2003, 28: 96
14. Nakajima T., Opt. Lett., 2000, 25: 847
15. Lukin M. D., et al., Phys. Rew. A,1999, 60 : 3225
16. Niu Yueping, et al., Opt. Lett., 2005, 30: 3371
17. Wang H., Goorskey D. J., and Xiao M., J. Mod. Opt., 2001, 49: 335
18. Schmidt H. and Imamoglu A., Opt. Lett.,1996, 21: 1936
19. Agarwal G. S., Quamtum Statistical Theories of Spontaneous Emission and Their Relation to Other Approaches, edited by Hohler G., Springer Tracts in Modern Physics, 1974: 70
20. Zhu S. Y and Scully M. O, Phys. Rev. Lett.,1996, 76: 388
21. Paspalakis E., Kylstra N. J., and Knight P. L., Phys. Rev. Lett., 1999, 82: 2079
22. Joshi A., Wang W., and Xiao M., Phys. Rev. A, 2003, 68: 015806
23. Gong S.-Q., Paspalakis E., and Knight P. L., J. Mod. Opt., 1998, 45: 2433
24. Ficek Z. and Swain S., J. Mod. Opt., 2002, 49: 3
25. Menon Sunish and Agarwal G. S., Phys. Rev. A, 1998, 57: 4014
26. Niu Yueping and Gong Shangqing, Phys. Rev. A , 2006, 73: 053811
27. M. O. Scully, Phys. Rev. Lett., 1985, 55: 2802
28. Evers J., Bullock D., and Keitel C. H., Opt. Commun., 2002, 209: 173
29. Pan J.-W. and Zeilinger A., Phys. Rev. A ,1998, 57: 2208
30. Qian J., Feng X.-L., and Gong S.-Q., Phys. Rev. A, 2005, 72: 052308
31. Qian J., Qian Y., Feng X.-L., Yang T., and Gong S.-Q., Phys. Rev. A, 2007, 75: 032309
32. Waks E. and Vuckovic J., Phys. Rev. Lett., 2006, 96: 153601